Biochimica et Biophysica Acta, 977 (1989) 40–51
Elsevier

BBABIO 43059

Spectroscopic studies of cyanobacterial phycobilisomes lacking core polypeptides

Patricia Maxson [1], Kenneth Sauer [1], Jianhui Zhou [2], Donald A. Bryant [2] and Alexander N. Glazer [3]

[1] *Department of Chemistry and Chemical Biodynamics Division, Lawrence Berkeley Laboratory, University of California Berkeley, CA,* [2] *Department of Molecular and Cell Biology, Penn State University, University Park, PA and* [3] *Department of Microbiology and Immunology, University of California, Berkeley, CA (U.S.A.)*

(Received 2 March 1989)
(Revised manuscript received 16 June 1989)

Key words: Phycobilisome mutant; Allophycocyanin-B deletion; Energy transfer

***Synechococcus* sp. PCC 7002 (*Agmenellum quadruplicatum* PR6) genes encoding two highly conserved phycobilisome core polypeptides, a small linker polypeptide (L^8_C, *apcC*) and the allophycocyanin-B α-subunit (α^{APB}, *apcD*), respectively, were interrupted by insertion of restriction fragments carrying the neomycin phosphotransferase gene of Tn5. The interrupted genes were used to transform *Synechococcus* sp. PCC 7002 to kanamycin resistance. The *apcC*$^-$ mutant assembled phycobilisomes lacking the L^8_C polypeptide and the *apcD*$^-$ mutant assembled phycobilisomes lacking α^{APB}. No other differences between the compositions of the mutant and wild-type phycobilisomes were detected. The *apcC*$^-$ strain grew about 25% more slowly than the wild-type, and its phycobilisomes dissociated more rapidly in 0.33 M Na/K-PO_4 (pH 8.0) or in 0.75 M Na/K-PO_4 at pH 8.0, at 40 °C, than did those of the wild-type. The phycobilisomes of this mutant were indistinguishable from those of the wild-type with respect to absorption and circular dichroism spectra, as well as time-resolved fluorescence emission. Steady-state emission spectra indicate a small decrease in long wavelength (680 nm) emission from the *apcC*$^-$ phycobilisomes and a complementary increase in shorter wavelength (665 nm) emission, relative to wild-type phycobilisomes. Strain *apcD*$^-$ phycobilisomes appear to be functionally indistinguishable from those of the wild-type, in spite of the absence of the two α^{APB} subunits which bear terminal acceptor bilins. The only spectroscopic difference was seen in the steady-state fluorescence emission, for which the emission of the mutant was about 15% higher than that of the wild-type and was slightly blue-shifted. A phenotype has yet to be found for the *apcD*$^-$ mutation.**

Introduction

The phycobiliproteins are a family of light-harvesting chromoproteins in the photosynthetic apparatus of cyanobacteria and red algae. The covalently attached prosthetic groups on these proteins are open-chain tetrapyrroles (bilins) [1]. These proteins are organized into macromolecular complexes, phycobilisomes, which form regular arrays on the cytoplasmic face of the thylakoid membranes [2]. The phycobilisome contains both phycobiliproteins and a set of linker polypeptides which determine the aggregation state and position of the various phycobiliproteins. Certain of the linker polypeptides influence the energy transfer within the phycobilisome through modulation of the spectroscopic properties of the phycobiliproteins or through the presence of bilin chromophores on the linker polypeptides themselves [3]. The spectroscopic properties of the phycobiliprotein subassemblies within the phycobilisome and their relative arrangement favor directional excitation energy transfer toward four terminal acceptor bilins [1].

The location of the various components of the phycobilisome has been determined in some detail for the phycobilisomes of *Synechococcus* sp. PCC 6301 [4–8], and *Synechocystis* sp. PCC 6701 [9,10]. The phycobilisomes of *Synechococcus* sp. PCC 7002 (*Agmenellum quadruplicatum* PR-6), the subject of this study, are morphologically similar to those of *Synechocystis* sp. PCC 6701. The polypeptide composition of

Abbreviations: PVDF, polyvinylidene difluoride; SDS, sodium dodecyl sulfate.

Correspondence: A.N. Glazer, Department of Microbiology and Immunology, University of California, Berkeley, CA 94720 (U.S.A.)

these phycobilisomes is given in Table I [11]. The genes encoding several of the components of the *Synechococcus* sp. PCC 7002 phycobilisome have been mutagenized by cartridge mutagenesis and the phenotypes of the resulting mutants analyzed [11]. The diagram (see Fig. 1) showing the locations of the various polypeptides within these phycobilisomes is based on these studies and on the assumed analogy to the structure of *Synechocystis* sp. PCC 6701 phycobilisomes.

Phycocyanobilin is the only bilin present in the *Synechococcus* sp. PCC 7002 phycobilisomes. The distinctive spectroscopic properties of the various complexes within the phycobilisome arise as a consequence of the various protein-bilin and bilin-bilin interactions. In the energy transfer path in *Synechococcus* sp. PCC 7002 phycobilisomes, excitation energy migrates from the phycocyanin hexamers (λ_{max}^{abs} 625–630 nm) of the rods (Fig. 1) to the allophycocyanin complexes (λ_{max}^{abs} 650 nm) of the core, and thence to two types of terminal acceptors, α^{APB} (λ_{max}^{abs} 670 nm) and L_{CM}^{99} (λ_{max}^{abs} 670 nm), in the core. As might be anticipated, *Synechococcus* sp. PCC 7002 mutants in which the α^{AP} and β^{AP} genes have been interrupted no longer form phycobilisomes [11]. Surprisingly, mutants in which the L_C^8 or α^{APB} genes have been interrupted grow photosynthetically at rates similar to or slightly reduced from that of the wild-type, and still assemble phycobilisomes which appear of normal size and polypeptide composition, lacking only the product of the interrupted gene. The comparison presented here of the properties of such 'incomplete' phycobilisomes with those of the wild-type permits some conclusions to be reached concerning the functions of L_C^8 and α^{APB}.

TABLE I

Estimated composition of the phycobilisomes of Synechococcus sp. PCC 7002

From Ref. 11. The molecular mass of the 99 kDa core polypeptide was calculated from the DNA sequence of the gene that encodes this component. The numbers in this table represent composite data accumulated from spectroscopic measurements, densitometric scans of stained polyacrylamide gels (both one- and two-dimensional) and unstained isoelectric focussing gels, and direct counts of the number of phycocyanin hexamers per peripheral rod by electron microscopy (Bryant, D.A., unpublished data). The ratio of phycocyanin to allophycocyanin determined by these methods for the wild-type was 1.96:1. Densitometric scans of SDS-polyacrylamide gels gave an approximate ratio of the 8, 8.5, 33, 29 and 99 kDa linker polypeptides of 1:1:1:1:0.32. The amounts of α^{APB} and β^{18} polypeptides were equal as determined from the densitometry of unstained and stained isoelectric focussing gels; the measured ratio of these subunits to the α or β subunit of allophycocyanin was 1:10–12. The close correspondence of these values to those more carefully determined for the phycobilisomes of *Synechocystis* sp. PCC6701 [9,10], which also have tricylindrical cores, indicates that the core compositions of these two species of phycobilisomes are similar if not identical. Consequently, the integral values in this table are based on the measured ratios, the assumption that each rod is composed of exactly two phycocyanin hexamers, and the proposed composition for tricylindrical phycobilisome cores as established in Refs. 4–10. For definition of abbreviations, see legend to Fig. 1.

Subunit	Copies/phycobilisome
Rod components:	
α^{PC}	72
β^{PC}	72
$L_R^{8.5}$	6
L_R^{33}	6
L_{RC}^{29}	6
Core components:	
α^{AP}	32
β^{AP}	34
α^{APB}	2
β^{18}	2
L_C^8	6
L_{CM}^{99}	2

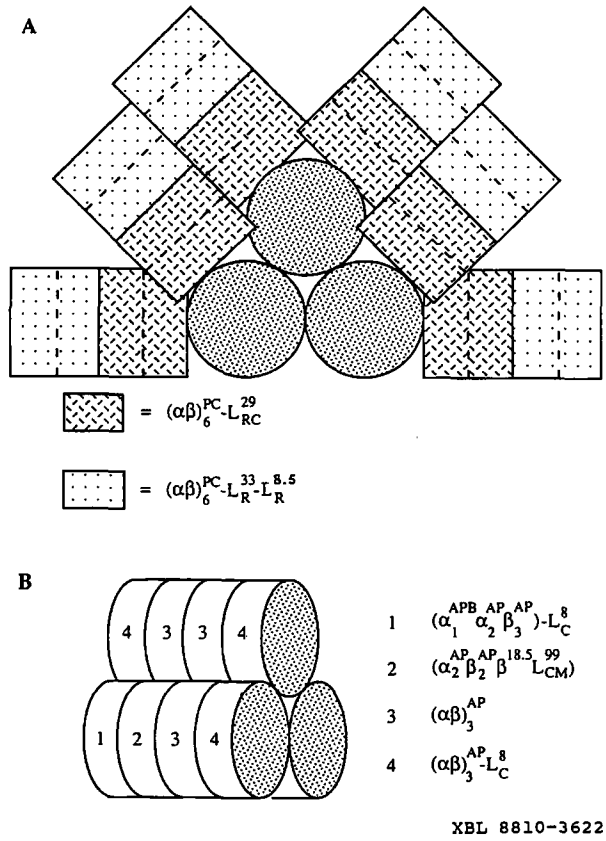

Fig. 1. Schematic representation of the phycobilisome of *Synechococcus* sp. PCC 7002. A rod is made up of two hexameric biliprotein complexes, each of which is attached through its specific linker polypeptide to the component adjacent to it in the phycobilisome. The manner in which the core cylinders are held together is not known. The abbreviations AP, APB, and PC are used for the biliproteins allophycocyanin, allophycocyanin B, and phycocyanin, and α^{AP}, β^{AP}, etc., for the α and β subunits of these proteins. Linker polypeptides are abbreviated L, with the superscript denoting the size in kDa, and a subscript that specifies the location of the polypeptide: R, rod substructure; RC, rod-core junction; C, core; CM, core-membrane junction. For other details, see Refs. 3 and 11. The arrangement shown for the core complexes is one of those suggested by Anderson and Eiserling [8].

Materials and Methods

Strains. *Synechococcus* sp. PCC 7002 (formerly *Agmenellum quadruplicatum* strain PR-6) was grown at 39° C under cool-white fluorescent illumination (about 250 $\mu E\ m^{-2} \cdot s^{-1}$) in medium A containing 1 $mg \cdot ml^{-1}$ $NaNO_3$ [12]. Carbon dioxide was supplied by bubbling the culture continuously with 1% CO_2/99% air. Mutant strains encoding the neomycin phosphotransferase of Tn5 were selected and maintained on media supplemented with 200 $\mu g \cdot ml^{-1}$ kanamycin. Solid media were prepared by solidifying the appropriate medium with 1.5% agar. DNA manipulations in *Escherichia coli* were performed in strain DH5α ($F^- \phi 80$ d*lacZ* ΔM15 Δ(*lacZYA-argF*) U169 *recA1 endA1 hsdR17* ($r_k^- m_K^+$) *supE*44 λ^- *thi-1 gyrA relA1*).

Large scale cultures for phycobilisome isolation were grown in medium A^+ [13] under 3% CO_2/97% N_2 and 200 $\mu E\ m^{-2} \cdot s^{-1}$ with constant stirring at 37° C. The *apcC*$^-$ and *apcD*$^-$ mutants were grown under similar conditions, except that NH_4Cl was substituted for $NaNO_3$ and 80 $\mu g \cdot ml^{-1}$ kanamycin was added to the growth medium to prevent reversion to the wild-type. Wild-type cells were always grown concurrently with the mutants. The *apcD*$^-$ mutant grew at the same rate as the wild-type, whereas the *apcC*$^-$ mutant grew at a rate about 25% slower. At 37° C, under 1% CO_2 in air, at 240 $\mu E\ m^{-2} \cdot s^{-1}$, the wild-type grew at 4.25 h/generation, and at 110 $\mu E\ m^{-2} \cdot s^{-1}$ at 7.75 h/generation, while under the corresponding conditions, the *apcC*$^-$ strain grew at 5.75 and 10.3 h/generation, respectively.

DNA isolation, partial library constructions, and other DNA manipulations. Total genomic DNA from *Synechococcus* sp. PCC 7002 was prepared as previously described [14]. Partial libraries of restriction fragments were constructed by ligating purified, size-fractionated restriction fragments (separated by preparative agarose gel electrophoresis) into appropriately digested plasmid vectors pMK3 [15], or pUC9 [16]. Libraries were screened by hybridization with the high-density colony filter method [17] or with re-gridded colonies replicated onto nitrocellulose filters. DNA fragments used as hybridization probes were prepared by preparative restriction endonuclease digestion and fractionated by agarose gel electrophoresis. The desired DNA fragments were excised from the gel, electroeluted into hydroxyapatite, eluted with 2.0 M potassium phosphate buffer (pH 7.0), containing 1.0 mM EDTA, desalted, and lyophilized [18]. Labelling of DNA fragments with α[^{32}P]dATP was performed by nick-translation [19] or by the random hexanucleotide-primers method [20]. Other DNA manipulations were carried out by routine methods [19,21,22].

Transformation of *Synechococcus* sp. PCC 7002 was performed as described [12]. Purified linear DNAs were used in all transformations at a concentration of approx. 1 $\mu g \cdot ml^{-1}$. Transformants were selected on medium A including 1 $mg \cdot ml^{-1}$ $NaNO_3$ and 200 $\mu g \cdot ml^{-1}$ kanamycin.

Construction of an apcC mutant of Synechococcus sp. PCC 7002. Clones encoding the *apcABC* locus of *Synechococcus* sp. PCC 7002 were identified by low-stringency, heterologous hybridization (see Refs. 18 and 23). The hybridization probe employed was a 1.3 kbp *Bam*HI-*Bgl* II DNA fragment which encodes the *apcAB* locus of the cyanelle genome of *Cyanophora paradoxa*

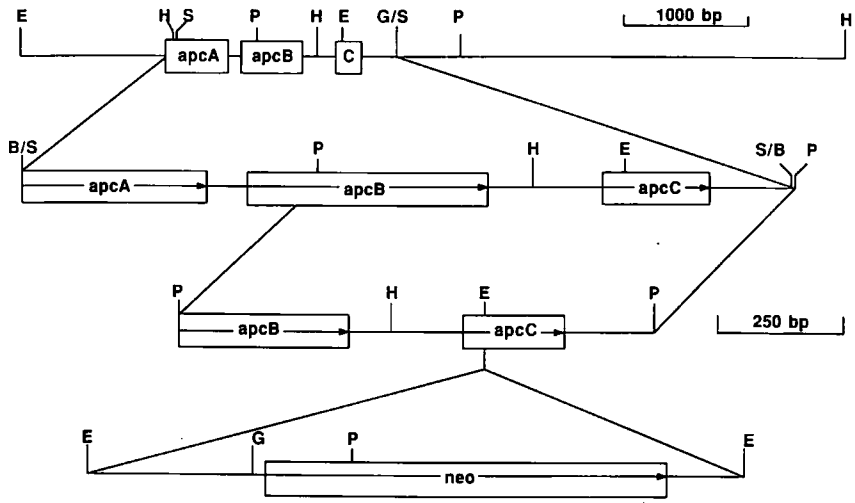

Fig. 2. Restriction map of the chromosomal *apcABC* locus of *Synechococcus* sp. PCC 7002 and of the cloned fragments employed in the construction of an *apcC* interruption mutant. The *Sau*3AI fragment encoding most of the *apcA, apcB,* and *apcC* genes was isolated from a library constructed in plasmid vector pMK3. The *Pst*I fragment encoding a portion of *apcB* and *apcC* was recloned in pUC9. A fragment encoding the neomycin phosphotransferase (*neo*) of Tn5 was then cloned into the *Eco*RI site situated at codons 15–17 of the *apcC* gene as shown. The *Pst*I fragment carrying the interrupted *apcC* gene was isolated and used to transform *Synechococcus* sp. PCC 7002 to kanamycin resistance. Restriction enzyme symbols: E., *Eco*RI; H, *Hin*dIII; S, *Sau*3AI; P, *Pst*I; G, *Bgl*II; B, *Bam*HI.

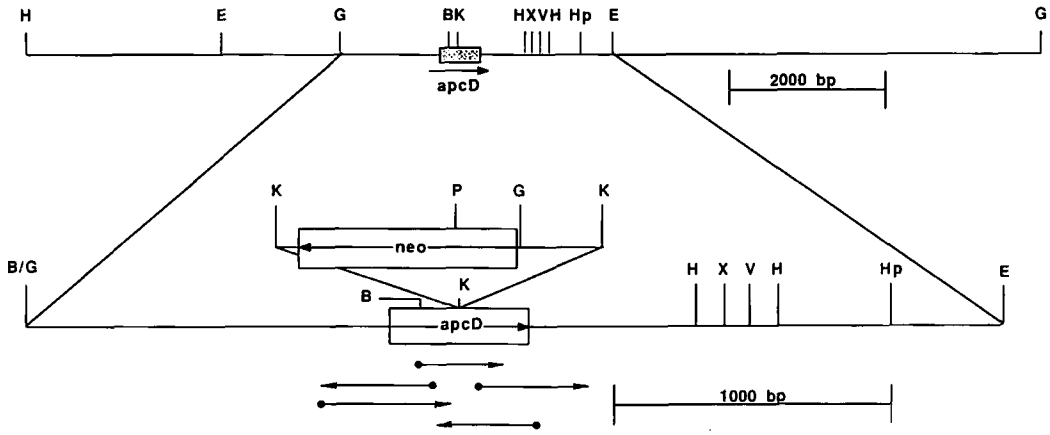

Fig. 3. Restriction maps of the chromosomal *apcD* locus of *Synechococcus* sp. PCC 7002 and the DNA construction employed in the creation of an *apcD* interruption mutant. The *apcD* coding region was cloned as two overlapping DNA fragments. The first clone contained the *Bam*HI-*Eco*RI fragment inserted in the same sites in plasmid pUC9. Sequence analysis revealed that the *Bam*HI site occurred in the *apcD* coding sequence, and the overlapping *Hin*dIII-*Bgl*II fragment was cloned into the *Hin*dIII and *Bam*HI sites of plasmid pUC9. The *apcD* gene was interrupted by cloning a *Kpn*I fragment encoding the neomycin phosphotransferase (*neo*) of Tn5 into the unique *Kpn*I site at codons 87–89 of the *apcD* gene as shown. The *Bam*HI-*Eco*RI fragment carrying the insertion was used to transform *Synechococcus* sp. PCC 7002 to kanamycin resistance. For additional details, see text. Restriction enzyme symbols: H, *Hin*dIII; E, *Eco*RI; G, *Bgl*II; B, *Bam*HI; K, *Kpn*I; X, *Xba*I; V, *Pvu*II; Hp, *Hpa*I; P, *Pst*I.

[23]. Two clones were isolated: the first was a 2.5 kbp *Eco*RI fragment which was shown by nucleotide sequencing to encode all of *apcAB* as well as the 5′ portion of *apcC* (see Fig. 2); the second clone contained a 1.75 kbp *Sau*3AI fragment which encoded a portion of *apcA* and all of *apcB* and *apcC* (see Fig. 2). The complete nucleotide sequence of the *apcABC* coding region, as well as flanking sequences (1.992 kbp in total) has been determined. A complete description of the nucleotide sequences, transcriptional analyses, and the construction of an *apcAB* deletion mutant will be published elsewhere (Stirewalt and Bryant, unpublished data).

A portion of the *apcABC* locus was re-cloned as a *Pst*I fragment in plasmid pUC9 as shown in Fig. 2. The resultant plasmid was partially digested with *Eco*RI and a 1.3 kbp *Eco*RI fragment, derived from plasmid pRL170 (C.P. Wolk and J. Elhai, personal communication), encoding the neomycin phosphotransferase of Tn5 was ligated into the plasmid as shown in Fig. 2. The *Pst*I fragment carrying the interrupted *apcC* gene was isolated and used to transform *Synechococcus* sp. PCC 7002 to kanamycin resistance. The resultant transformants were subjected to several rounds of purification by streaking on selective medium, and individual colonies were tested for the configuration of their DNAs at the *apcC* locus by Southern blot hybridization.

Construction of an apcD mutant of Synechococcus sp. PCC 7002. The *apcD* gene of *Synechococcus* sp. PCC 7002 was cloned by low stringency hybridization [18] by using the 1.060 kbp *Hin*dIII fragment encoding most of the *apcAB* genes of *Synechococcus* sp. PCC 7002 as probe (see Fig. 2). A 1.6 kbp *Eco*RI-*Bam*HI fragment was found to hybridize weakly to this probe on genomic Southern blots, and this fragment was cloned from a size-fractionated partial library constructed in plasmid pUC9. Nucleotide sequence analysis of a portion of this clone revealed that the *Bam*HI site occurred within the coding sequence of the *apcD* gene near the 3′ terminus of the gene (see Fig. 3). An overlapping *Hin*dIII-*Bgl*II restriction fragment of 2.4 kbp was cloned from a partial pUC9 library to provide the remaining *apcD* gene sequences. The *apcD* gene was inactivated by insertion of a 1.3 kbp *Kpn*I fragment, derived from plasmid pRL171 (C.P. Wolk and J. Elhai, personal communication) and encoding the neomycin phosphotransferase gene of Tn5, into the unique *Kpn*I site occurring at codons 87–89 of the *apcD* gene as shown in Fig. 3. The interrupted *apcD* gene was isolated as a *Hin*dIII fragment and used to transform *Synechococcus* sp. PCC 7002 to kanamycin resistance. Resultant transformants were selected and purified by repeated streaking on selective medium to allow segregation to occur. Selected colonies were tested for the configuration of their DNAs at the *apcD* locus by Southern blot hybridization. A more complete description of the molecular cloning, nucleotide sequence analysis, transcriptional analysis, and mutant construction, confirmation, and characterization will be presented elsewhere (Zhou, J., Stirewalt, V.L. and Bryant, D.A., unpublished data).

Phycobilisome preparation. Phycobilisomes were prepared by a procedure similar to that described by Yamanaka et al. [24]. All buffers contained 1 mM NaN_3 and 20 μM phenylmethanesulfonyl fluoride. All preparative procedures were carried out at room temperature. Phycobilisomes of the mutants and wild-type were always prepared at the same time. Cells were harvested

when the cell density was approx. 1.5–2.0 g/l and resuspended to 0.12 $g \cdot ml^{-1}$ in 0.65 M NaH_2PO_4/K_2HPO_4 (Na/K-PO_4) buffer (pH 8.0). In this buffer, the cells were homogenized and broken by four passages through a French pressure cell at 124 MPa. The broken cells were incubated in 1.2% Triton X-100 for 30 min and then centrifuged at 16000 rpm in a Sorvall SS-34 rotor for 30 min. The supernatant from this spin was drawn off and loaded onto sucrose step gradients consisting of equal volumes of 0.2, 0.4, 0.6, 0.8 and 1.0 M sucrose in 0.75 M Na/K-PO_4 buffer (pH 8.0) for a total volume of 38 ml. The gradients were centrifuged in a Beckman SW-27 rotor at 21000 rpm for 16 h at 18° C. Most spectroscopic measurements were made within 10 h of recovery of the phycobilisomes from the gradients.

Polyacrylamide gel electrophoresis. Gel electrophoresis was performed on 0.75 mm thick slab gels by the method of Laemmli [25] with equipment from Hoeffer Scientific (San Francisco, CA). The running gels were 15% and the stacking gels 6% acrylamide. To detect the L_C^8 polypeptide, 45 μg of total protein was loaded onto each lane. Because of the high salt concentration of the buffers, the proteins were precipitated in 10% trichloroacetic acid for a minimum of 1 h at 4° C before addition of the gel solubilization mixture. The gels were run at 30 mA constant current until the tracking dye in the solubilization mixture just ran off the gel. The gels were treated with either Coomassie brilliant blue or a silver-stain preparation.

Two-dimensional gel electrophoresis procedure was that of O'Farrell [26]. The first dimension isoelectric focusing gels were cast in 3 mm (inner diameter) tubes and were run with a 4:1 combination of pH 4–6/pH 3–10 ampholyte. Gels were focussed for 12 h at 400 V. The second dimension was performed on a slab gel as described above. In this case the tube gel was laid across the top of the slab and sealed in place with hot agarose solution.

Amino acid sequence determination. The sequences of the low molecular mass polypeptides (approximately 8 kDa) from the phycobilisomes of the *apcC*$^-$ mutant and the wild-type were determined from electroblotted films of polyvinylidene difluoride (PVDF) according to the method of Matsudaira [27]. The quantity of wild-type phycobilisomes containing 250 picomoles of L_C^8 was calculated based on the assumption that there are two copies of phycocyanin hexamer per L_C^8 and that $\varepsilon^{600}_{nm} = 6.7\ ml \cdot mg^{-1} \cdot cm^{-1}$ for phycobilisomes [28]. Using a molecular mass of 250 kDa for the phycocyanin hexamer plus linker, this corresponded to 120 μg of protein. The same amount of material from *apcC*$^-$ phycobilisomes was used as from those of the wild-type. Electrophoresis was performed as described above. After electrophoresis, the gel was soaked in transfer buffer (10 mM 3-(cyclohexylamino)-1-propanesulfonic acid, 10% methanol (pH 11)) for 5 min. The gel was then sandwiched between a film of PVDF, which had been rinsed with 100% methanol, and several sheets of blotting paper. The assembly was placed in a blotting apparatus and electroeluted for 30 min at 0.5 A in transfer buffer. Afterwards, the PVDF film was washed in deionized H_2O for 5 min, stained with 0.1% Coomassie brilliant blue in 50% methanol for 5 min, destained in 50% methanol, 10% acetic acid for 5–10 min, then finally rinsed in deionized H_2O for 5–10 min and allowed to air dry. The desired bands were cut out of the PVDF film for sequence analysis. Peptides from the film were sequenced in an automated gas-liquid solid-phase sequenator (Model 477A, Applied Biosystems, Foster City, CA) [29].

Spectroscopic measurements. Absorption measurements were made with a Varian 2300 UV-Visible Spectrophotometer (Varian, Houston, TX). Circular dichroism measurements were made with a Jasco J-500 Spectro-polarimeter on samples with a known absorbance between 1.0 and 1.3 cm^{-1} at λ_{max}.

Steady-state fluorescence emission spectra were taken with a SPEX Fluorolog 2 model 212 spectrofluorimeter (SPEX Industries, Metuchen, NJ) interfaced with an Epson Equity I computer through a Fluorometer Control System (Brown's Software, Penllyn, PA). The detector used was a cooled RCA 31034A photomultiplier tube. The dark noise from the photomultiplier tube was subtracted from all measurements. Monochromator slits were adjusted such that the intensity of emitted light fell into a range favorable for photon counting (100000–300000 cps) which led to a bandwidth range of 1–2 nm. The wavelength dependence of the fluorimeter was corrected by calibration with a standard lamp (Optronics Laboratories 245C). All measurements were made with detection at 90° to excitation. The maximum absorption of the samples was 0.2 cm^{-1} for all steady-state emission experiments. Polarization measurements were made with Glan Thompson polarizers. For emission polarization, the samples were excited at 590 nm; for excitation polarization, the emission was monitored at 720 nm. For the ionic strength and temperature studies, samples were diluted by direct introduction of the material into the cuvette used for measurement followed by rapid mixing by hand. During the temperature studies the cuvette containing the diluting buffer was allowed to equilibrate at the temperature of interest before introduction of the room temperature sample. The dilution of the sample was always by at least a factor of forty, ensuring that the final temperature was close to that of the diluting buffer. The temperature of the sample was controlled with a temperature regulating recirculating bath (Neslab RTE-5B).

Picosecond pulses for the time resolved measurements were provided by a tunable, cavity-dumped dye laser using rhodamine 6 G as the lasing dye (Spectra Physics model 375, Mountain View, CA) synchronously

pumped by an argon ion laser (Spectra Physics, model 171). The excitation beam was vertically polarized and the fluorescence emission from the samples was monitored at the magic angle to eliminate anisotropic artifacts in the decay components. The emission wavelength was selected by a double monochromator (Instruments SA, Metuchen, NJ) with a 4 nm bandwidth. Data were collected from an ITT microchannel plate detector (model F4129) using the single-photon timing technique and were analyzed as sums of exponential decays using an iterative deconvolution program. The time resolution of the instrument, limited by the response of the detector, was around 20 ps. Measurements were taken with a 2×3 mm cuvette with samples that had an effective maximum absorbance of 0.27.

Results

Characterization of the transformants

Transformation of *Synechococcus* sp. PCC 7002 with the *apcC* gene interrupted by a DNA fragment encoding the neomycin phosphotransferase of Tn5 (see Fig. 2) resulted in kanamycin-resistant, *apcC*$^-$ colonies after segregation. Southern blot hybridization analyses of selected transformants revealed that the *apcC* locus was interrupted in all cases and that the mutants were homozygous (Fig. 4). When the DNAs of transformants were digested with *Hin*dIII and probed with the 0.933 kbp *Pst*I-*Bgl*II fragment encoding a portion of *apcB* and *apcC*, two fragments of 1.060 kbp and 5.5 kbp hybridized as predicted, while fragments of 4.2 kbp and 1.060 kbp were observed for the wild-type (Panel A, Fig. 4). A single fragment of 1.6 kbp is observed when the wild-type DNA is digested with *Pst*I and probed with the same DNA fragment (Panel B, Fig. 4). Two fragments of 1.9 and 1.0 kbp are observed when the DNAs of the transformants are digested with *Pst*I, since the inserted DNA carries a single *Pst*I site (see Fig. 2). These results confirm that the *apcC* gene is interrupted in the transformants. Similar Southern blot hybridization experiments were performed to confirm that the *apcD* gene was interrupted in the *apcD*$^-$ mutants (results not shown). The expected restriction fragments, differing in all cases from those of the wild-type, confirmed that homozygous *apcD*$^-$ mutants were obtained as expected.

Comparison of apcC$^-$ *mutant and wild-type phycobilisomes*

A diagrammatic representation of the sucrose density gradient step in the phycobilisome purification (see Materials and Methods) is shown in Fig. 5A. The phycobilisomes appear as dark blue bands in the 0.6 M sucrose region with the same sedimentation rate for both mutant and wild-type. In the 0.2 M sucrose region, both samples show a blue band varying in intensity

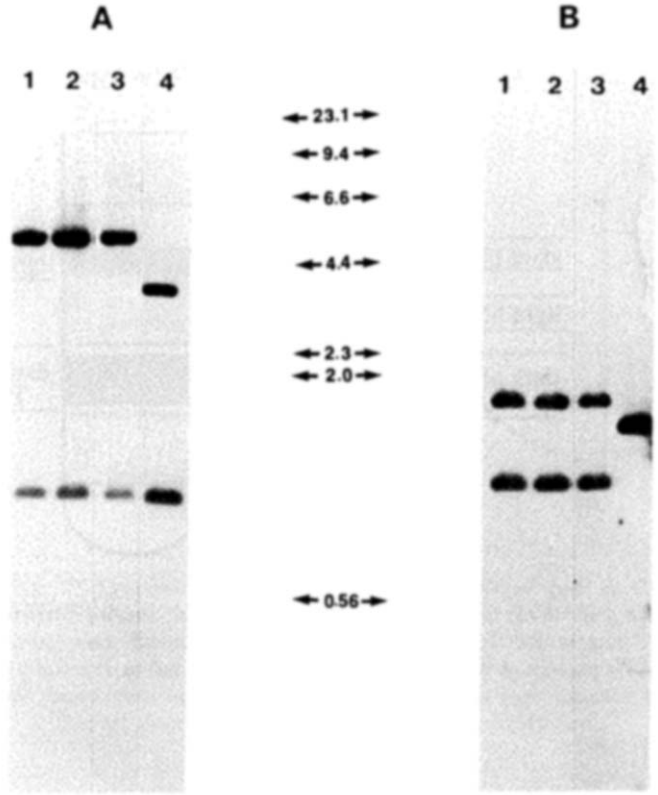

Fig. 4. Fluorogram of Southern plot hybridization experiment to confirm the interruption of the *Synechococcus* sp. PCC 7002 *apcC* gene. Total DNAs (chromosomal and plasmid DNAs) of the wild-type (Lane 4) and of three independent kanamycin-resistant mutant transformants (Lanes 1, 2 and 3) were digested with either *Hin*dIII (A) or *Pst*I (B) and electrophoresed on a 0.75% agarose gel. DNA fragments were transferred to a nitrocellulose filter by capillary action. The resultant filter was probed by hybridization with the 0.933 kbp *Pst*I-*Bgl*II fragment, encoding the 3′ portion of the *apcB* as well as the *apcC* gene (see Fig. 1), which had been labeled with ^{32}P by nick-translation. The numbered arrows indicate the positions of size markers, which were the *Hin*dIII fragments of bacteriophage lambda DNA, in kbp. For additional details, see text.

from preparation to preparation which consists of dissociated phycobilisomes. A middle blue band was always prominent in the *apcC*$^-$ phycobilisome gradients and virtually absent from wild-type gradients, and was shown by gel electrophoresis and spectroscopic measurements to be enriched in allophycocyanin relative to intact phycobilisomes (data not shown), indicating that it consisted predominantly of dissociated core components.

The phycobilisomes from the *apcC*$^-$ mutant were characterized in various ways to ensure that there was no change in polypeptide composition to compensate for the loss of the L^8_C polypeptide and to prove that this polypeptide was in fact missing from the mutant structures. There are two small polypeptides of similar molecular mass in *Synechococcus* sp. PCC 7002 phycobilisomes, L^8_C and $L^{8.5}_R$ [11]. The latter polypeptide, a rod 'capping' polypeptide, is located at the distal ends of the phycobilisome rods (see Fig. 1) and appears to

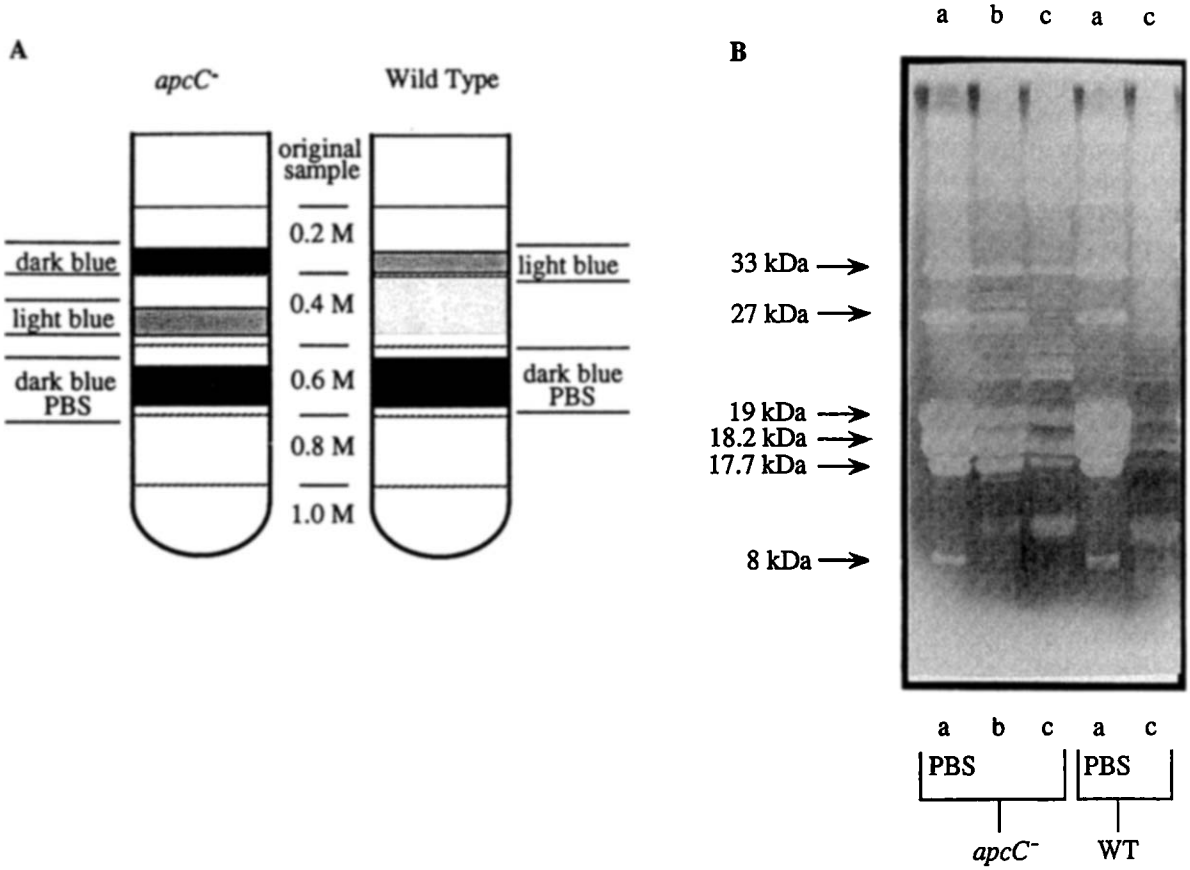

Fig. 5. Profiles of phycobilisome purification by sucrose density centrifugation from *Synechococcus* sp. PCC 7002 wild-type and the *apcC*$^-$ mutant. The lines indicate the boundaries of the sucrose layers before centrifugation. (B) Silver-stained SDS-polyacrylamide gel of wild-type and *apcC*$^-$ phycobilisome components. Lanes identified a, b and c correspond to the bottom, middle, and top bands indicated on the diagrams of the gradients in (A). WT, wild-type; PBS, phycobilisomes.

play a role in the stable attachment of the terminal phycocyanin trimer disc to the rods [11,30]. The L^8_C and $L^{8.5}_R$ polypeptides comigrate on SDS-polyacrylamide gels. Polyacrylamide gels of wild-type and mutant phycobilisomes, stained with Coomassie brilliant blue, both show a band in the region of 8 kDa, although the

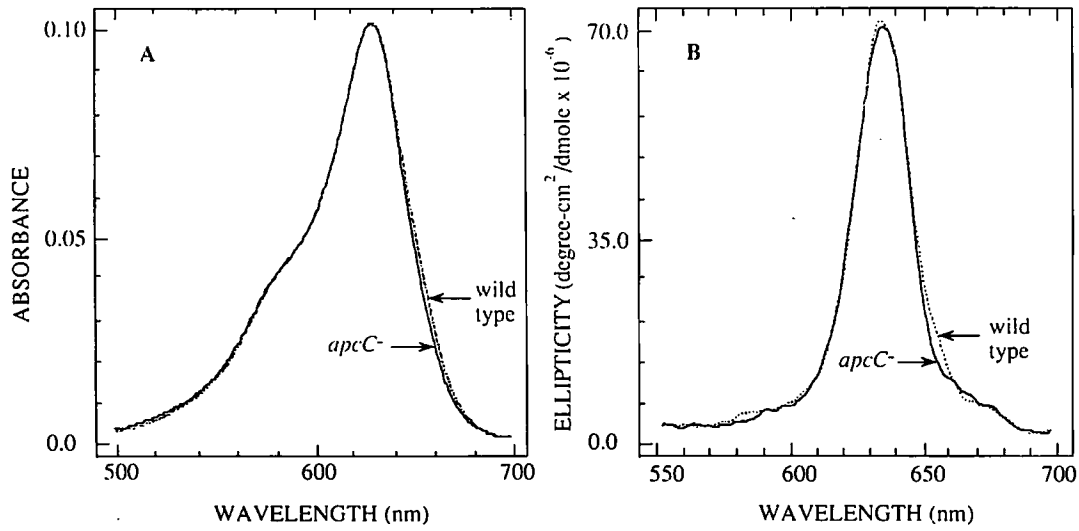

Fig. 6. Absorption (A) and circular dichroism (B) spectra of wild-type and *apcC*$^-$ phycobilisomes. Wild-type phycobilisome spectra are represented by dotted lines and those of the *apcC*$^-$ mutant by solid lines. For the CD spectra, samples were taken directly from the sucrose gradients and had absorbances between 10 and 12 cm^{-1} at the maximum (635 nm). Measurements were taken on undiluted samples in cells with a pathlength of 0.1 cm to give an effective absorbance between 1.0 and 1.2.

band in the mutant phycobilisome lane is much fainter than that in wild-type lane. The more sensitive silver stain procedure (Fig. 5B) shows clearly that polypeptides of about 8 kDa are present in both the mutant and wild-type structures. The bands in the 8 kDa region were electroblotted onto PVDF membranes and subjected to twelve rounds of sequential Edman degradation [31]. The amino acids released at each step were compared to those predicted by the DNA sequences of the *apcC* (encoding L_C^8) and *cpcD* (encoding $L_R^{8.5}$) genes [30]. The sequence results showed that only the $L_R^{8.5}$ polypeptide was present in the mutant phycobilisomes, whereas residues from both the L_C^8 and $L_R^{8.5}$ polypeptides were recovered from the wild-type phycobilisomes.

Two-dimensional gels were run with isoelectric focussing from pH 3 to 10 in the first dimension, to check for the presence of the other core polypeptides in the mutant and wild-type phycobilisomes, particularly the α^{APB} subunit [10,32]. The two-dimensional pattern of phycobiliprotein polypeptides was the same for wild-type and strain *apcC*$^-$.

Fig. 6A shows the absorption spectra of the mutant and the wild-type phycobilisomes. The greatest difference, about 5% of the total absorption, occurs at 658 nm. The CD spectra of the two complexes (Fig. 6B) are similar; there is a single positive feature with a maximum at 635 nm. The intensity at the maximum of the band is the same for wild-type and mutant; the only significant difference occurs between 650 and 670 nm, as in the absorption spectra. In that region, the CD spectrum of the *apcC*$^-$ phycobilisome is less positive than that of the wild-type.

The steady state fluorescence emission spectra are shown in Fig. 7. Emission spectra were independent of excitation wavelength between 580 and 640 nm for both types of phycobilisomes. The difference between the phycobilisomes is more pronounced in the fluorescence emission spectra than in the absorption or CD spectra. The wild-type has a maximum fluorescence at 680 nm whereas the mutant phycobilisome fluorescence is maximal at 665 nm. Fig. 7 provides a direct comparison of the quantum yields of fluorescence of the mutant versus the wild-type, because the absorptions of the two samples were matched at the excitation wavelength. As can be seen, there is very little difference in the fluorescence intensity at the maxima.

Both the excitation and emission polarization spectra yielded a polarization of 0.0 ± 0.1 across the range of wavelengths examined (for details, see Ref. 31). For excitation polarization, emission was monitored at 720 nm and the excitation monochromator scanned from 500 to 670 nm. For emission polarization, the samples were excited at 590 nm and the emission monochromator scanned between 600 and 750 nm. This depolarization is interpreted as arising from the large number of

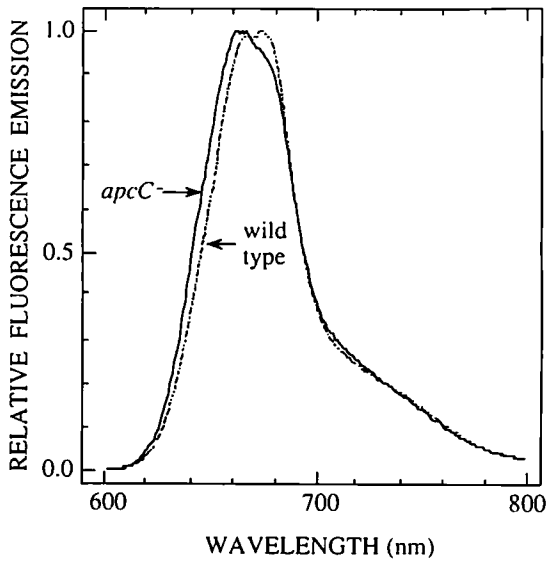

Fig. 7. Fluorescence emission spectra of wild-type and *apcC*$^-$ phycobilisomes. Samples in 0.6 M sucrose solution (from the gradients) were diluted into 0.75 M Na/K-PO_4 (pH 8.0) to give an absorbance of less than 0.2 cm^{-1} at λ_{max}. To allow direct comparison of fluorescence quantum yields, the two samples were matched to equal absorbance at the excitation wavelength (590 nm).

chromophores involved in the phycobilisome energy transfer and prevents detection of any differences in the core chromophore orientation of the mutant compared with the wild-type.

Phycobilisomes dissociate under conditions of low ionic strength or elevated temperature. The fluorescence of the wild-type phycobilisomes before and after dilution into 50 mM Na/K-PO_4 (pH 8), shows a shift in the maximum from 680 to 650 nm signalling a much greater contribution to the fluorescence from phycocyanin which is no longer connected to the core. The same effect can be produced by raising the temperature.

The dissociation of the phycobilisomes at lower ionic strength was examined by rapid dilution of the phycobilisome solutions (0.8 M sucrose, 0.75 M Na/K-PO_4) into phosphate buffers varying in concentration. The resulting dissociation was followed by sampling the fluorescence at 680 nm at 1 s intervals while exciting with 590 nm light. Kinetic traces of fluorescence from the wild-type and mutant phycobilisomes at 680 nm, after dilution into 0.65, 0.33 or 0.05 M Na/K-PO_4, are shown in Fig. 8A. Dilution into 0.65 M Na/K-PO_4 causes little decrease in fluorescence at 680 nm over 10 min in either complex, whereas dilution into 0.05 M Na/K-PO_4 causes a rapid decrease in fluorescence which is essentially complete after 2 min, again for both complexes. Differences between the wild-type and the mutant become apparent at 0.33 M Na/K-PO_4; in this buffer the wild-type phycobilisome 680 nm fluorescence decreases much more slowly than does that of the mutant phycobilisomes. The rate of decrease of the *apcC*$^-$ phycobilisome 680 nm fluorescence on dilution

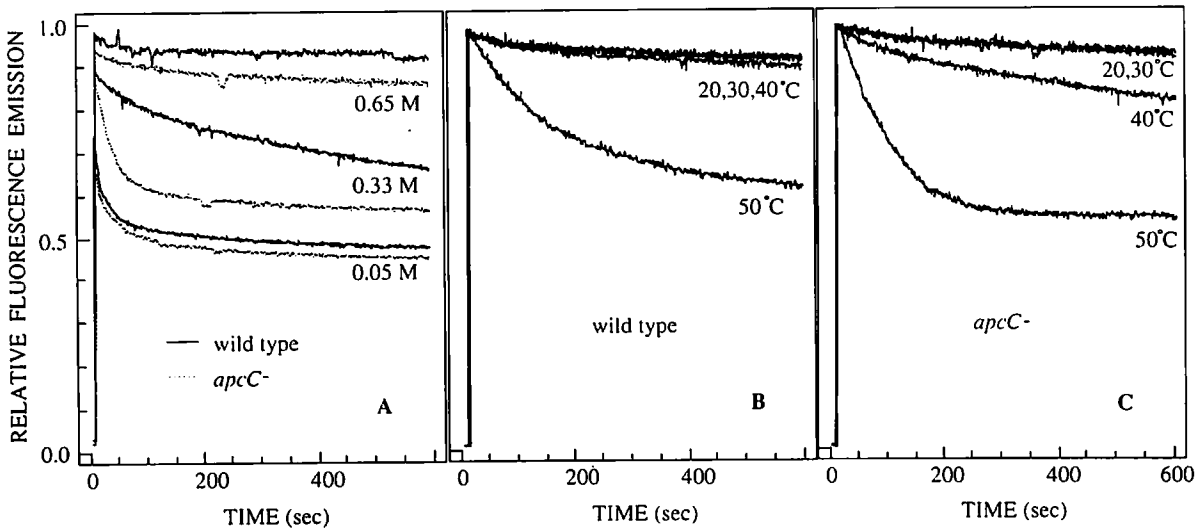

Fig. 8. Kinetics of fluorescence decay at 680 nm of *Synechococcus* sp. PCC 7002 wild-type and *apcC*$^-$ phycobilisomes after dilution into buffers of different concentrations or into the same buffer at different temperatures. Stock phycobilisome solutions, in 0.8 M sucrose, 0.75 M Na/K-PO_4 (pH 8.0), were diluted approximately 40-fold at time zero into the buffers indicated below. Precise dilutions were chosen to give closely matching sample absorptions at 590 nm after dilution. (A) Dilution into 0.65, 0.33, and 0.05 M Na/K-PO_4 (pH 8.0) at 20 ° C. The lower decay curve (dotted line) of each pair is that of the mutant phycobilisome fluorescence. (B) Dilution of wild-type phycobilisomes into 0.65 M Na/K-PO_4 (pH 8.0) at 20, 30, 40 or 50 ° C. (C) Dilution of *apcC*$^-$ phycobilisomes under conditions corresponding to those in (B). Excitation was at 590 nm for all measurements.

with 0.33 M Na/K-PO_4 is similar to that resulting from dilution into 0.05 M Na/K-PO_4 (Fig. 8A).

Figures 8B and 8C show the kinetics of dissociation of the phycobilisomes at 20, 30, 40, and 50 ° C. The wild-type shows little evidence of dissociation until the temperature is raised above 40 ° C; the mutant begins to dissociate at 40 ° C and shows more rapid dissociation at 50 ° C than the wild-type. After 10 min at 50 ° C the mutant and wild-type exhibit the same fluorescence spectrum, with a maximum at 655 nm. When the temperature is lowered to 20 ° C after measurement at 40 ° C, the wild-type fluorescence spectrum is recovered almost completely. After the wild-type phycobilisome has been exposed to 50 ° C, a small portion of the 680 nm peak is recovered when the temperature of the sample is lowered to 20 ° C. The recovery of the mutant phycobilisome fluorescence is not so great. After treatment at 40 ° C, the fluorescence maximum when measured at 20 ° C is still at 655 nm, and the shoulder at 680 nm increases by only 10–15%. There is no recovery of the fluorescence spectrum of the mutant at 20 ° C after heating to 50 ° C.

Comparison of apcD$^-$ *mutant and wild-type phycobilisomes*

The *apcD*$^-$ mutant phycobilisomes have the same sedimentation behavior on sucrose density gradients as

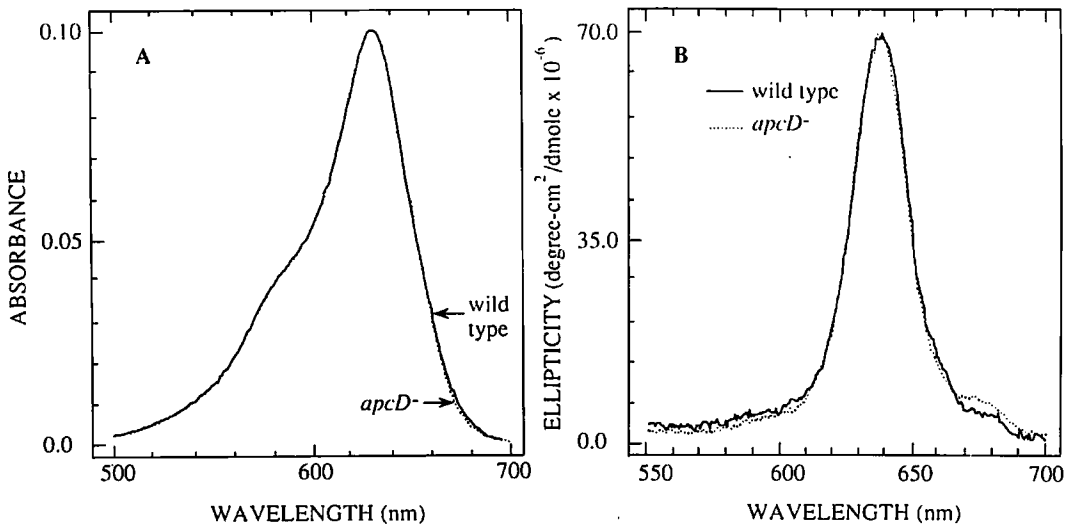

Fig. 9. Absorption (A) and circular dichroism (B) spectra of wild-type and mutant *apcD*$^-$ phycobilisomes. All conditions were as described in the legend to Fig. 6.

do the wild-type particles. The absorption spectra of both types of phycobilisomes are almost identical (Fig. 9A). The α^{APB} polypeptide can be readily resolved from the other components of the phycobilisome core by two-dimensional gel separation with isoelectric focusing in the first dimension and electrophoresis in the presence of SDS in the second dimension [4,10]. It was confirmed that by this criterion the *apcD*$^-$ mutant phycobilisomes were lacking in the α^{APB} polypeptide (data not shown). Between 655 and 685 nm the absorbance of the mutant phycobilisomes is slightly lower than that of the wild-type. The greatest difference between the two occurs at 670 nm and is approx. 2% of the maximum absorbance (at 632 nm). The CD spectra of both complexes (Fig. 9B) are very similar, displaying a positive feature with a maximum at 635 nm. These observations show that the deletion of the two α^{APB} polypeptides from the phycobilisome core has not altered the size of the structure or the conformation of the other components.

Fig. 10 shows the fluorescence emission of the mutant and wild-type phycobilisomes for samples which have equal absorbance at the excitation wavelength (590 nm). The maximum fluorescence emission for the mutant phycobilisomes occurs between 665 and 668 nm; the maximum emission of the wild-type occurs at 680 nm. The quantum yields of the two complexes were compared for a number of different samples; the fluorescence of the mutant phycobilisomes was 15 ± 20% higher than that of the wild-type particles.

No difference between mutant and wild-type phycobilisomes was seen in fluorescence decay measurements. Table II provides a summary of results for 625, 650 and 670 nm excitation of the mutant phycobilisomes. Deconvolution of wild-type phycobilisome fluorescence decay measurements yielded the same values. Time-resolved emission measurements performed on whole cells likewise revealed no significant differences between the wild-type and mutant for excitation at 625 and 670 nm, and emission monitored between 675 and 720 nm.

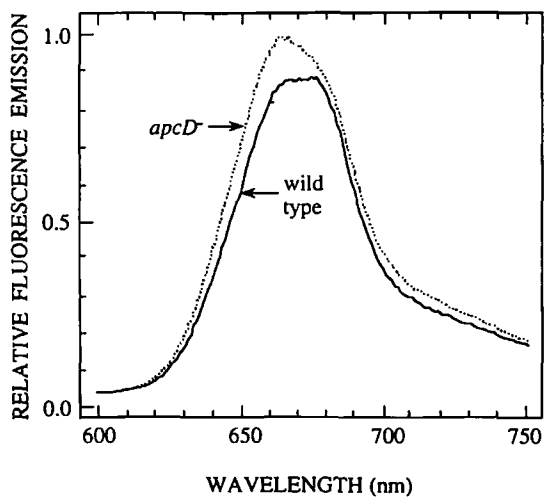

Fig. 10. Fluorescence emission spectra of wild-type and *apcD*$^-$ phycobilisomes. All conditions were as described in the legend to Fig. 7.

TABLE II

Time-resolved emission data for apcD$^-$ *phycobilisomes*

Exponential decay components of fluorescence emission at wavelength λ^{em} are characterized by an amplitude, α, and a decay time, τ. A negative value of the amplitude refers to an induction or rise component

625 nm excitation			
$\lambda^{em}_{660\ nm}$		$\lambda^{em}_{690\ nm}$	
α	τ (ns)	α	τ (ns)
0.41	1.7	1.5	1.7
0.09	0.26	0.26	0.50
0.50	0.03	−0.78	0.10
τ_{mean} = 1.6 ns [a]		τ_{mean} = 1.7 ns	
650 nm excitation			
$\lambda^{em}_{660\ nm}$		$\lambda^{em}_{690\ nm}$	
α	τ (ns)	α	τ (ns)
0.32	1.7	1.26	1.7
0.09	0.26	0.28	0.30
0.59	0.02	−0.54	0.08
τ_{mean} = 1.6 ns		τ_{mean} = 1.7 ns	
670 nm excitation			
$\lambda^{em}_{690\ nm}$			
α		τ (ns)	
0.24		1.7	
0.08		0.40	
0.68		0.02	
τ_{mean} = 1.6 ns			

[a] $\tau_{mean} = \Sigma_i \alpha_i \tau_i^2 / \Sigma_i \alpha_i \tau_i$

Discussion

Earlier studies of allophycocyanin complexes containing the L^8_C and/or the α^{APB} polypeptides were suggestive of specific roles for these core components (for a review, see Ref. 3). As shown in Fig. 1, the top cylinder of the core consists of four trimeric allophycocyanin complexes, two of which contain the small core polypeptide L^8_C. Two additional such complexes are present in each of the two basal cylinders for a total of six L^8_C-containing complexes (Table I). Earlier comparison of the properties of isolated $(\alpha^{AP}\beta^{AP})_3L^8_C$ and $(\alpha^{AP}\beta^{AP})_3$ complexes showed that their spectroscopic properties were similar [6], but that the $(\alpha^{AP}\beta^{AP})_3L^8_C$ complex was stable even at extreme dilution where the $(\alpha^{AP}\beta^{AP})_3$ complex dissociated to $\alpha^{AP}\beta^{AP}$ monomers [6,33]. The $(\alpha_1^{APB}\alpha_2^{AP}\beta_3^{AP})L^8_C$ complex is likewise resistant to dissociation [6]. On the basis of these observa-

tions, it was proposed that L_C^8 stabilizes allophycocyanin-containing trimers and prevents subunit exchange between the α^{APB}-containing complexes and those lacking this polypeptide [6].

Cells of the *apcC*$^-$ mutant assemble phycobilisomes of the same size and composition as those of the wild-type, except for the absence of L_C^8. The polypeptide pattern of the mutant phycobilisomes revealed by SDS-polyacrylamide gel electrophoresis (Fig. 5, and of gels stained with Coomassie brilliant blue [31]) indicates that the missing L_C^8 is not replaced by some other polypeptide (e.g., additional $L_R^{8.5}$). The 'incomplete' *apcC*$^-$ phycobilisomes are functionally indistinguishable from those of the wild-type. This is an unexpected finding. It was anticipated that the removal of six L_C^8 polypeptides from the phycobilisome core would have pronounced structural consequences. However, the incomplete phycobilisomes are less stable as indicated by more rapid dissociation at lower phosphate concentration or at elevated temperature (Fig. 8A–C). The *apcC*$^-$ mutant grows about 25% more slowly than the wild-type, both at low and high light intensity, suggesting that phycobilisomes may assemble less efficiently in this mutant and/or may be less stable. Support for the latter possibility is found in the presence of larger amounts of dissociated phycobilisome components in preparations of mutant as compared to wild-type phycobilisomes (Fig. 5). In sum, the results support the conclusion that L_C^8 contributes to phycobilisome stability in vivo and in vitro, but that it is not required for the correct assembly of the phycobilisome core.

Studies on separated phycobilisome components have established that the phycocyanobilins on the α^{APB} and L_{CM}^{99} polypeptides have the longest wavelength absorption maxima (670 nm) and fluorescence emission maxima (680 nm) of all of the bilins in the phycobilisome [33–37]. Consistent with these observations, studies of isolated *Synechococcus* sp. PCC 6301 $(\alpha_1^{APB}\alpha_2^{AP}\beta_3^{AP})L_C^8$ and $\alpha_2^{AP}\beta_2^{AP}\beta^{18.5}L_{CM}^{75}$ complexes showed that α^{APB} and L_{CM}^{75} serve as terminal energy acceptors within these complexes [5,6,38,39]. From examination of the absorption and steady state fluorescence emission properties of *Nostoc* sp. phycobilisomes, Zilinskas et al. [40] and Mimuro et al. [41] concluded that energy transfer from allophycocyanin to α^{APB} or to L_{CM}^{94} (corresponding to L_{CM}^{99} in *Synechococcus* sp. PCC 7002) occurs independently. A similar conclusion was reached by Gillbro et al. [42] from time-resolved studies of fluorescence decay at 680 nm in *Synechococcus* sp. PCC 6301 strain AN112 phycobilisomes.

Deletion of the α^{APB} polypeptide does not affect phycobilisome assembly or the growth rate of *Synechococcus* sp. PCC 7002. It can be inferred that the bilins on the two L_{CM}^{99} polypeptides are sufficient for the mediation of energy transfer between the phycobilisome and the chlorophyll *a*-containing complexes of the thylakoid membrane with scarcely altered overall efficiency. In other words, the orientations and distances between the 24 phycocyanobilins within each of the two basal cylinders of the phycobilisome core are such that efficient transfer to the remaining single acceptor bilin can take place.

The amino acid sequences of α^{APB} and of α^{AP} from diverse cyanobacteria are 52–55% identical [11,43,44]. In vitro, when the $(\alpha^{AP}\beta^{AP})_3$ and $(\alpha^{APB}\beta^{AP})_3$ complexes are mixed, rapid subunit exchange leads to the formation of a mixture of the four possible complexes in near-statistical proportions [33]. This observation indicates that the contacts between α^{AP} and β^{AP} subunits are similar to those between α^{APB} and β^{AP} subunits. A plausible suggestion is that the α^{APB} polypeptides in the core of the *apcD*$^-$ mutant phycobilisomes are replaced by α^{AP} polypeptides.

The only significant difference in the spectroscopic properties of the wild-type and the strain *apcD*$^-$ phycobilisomes is in the steady-state fluorescence emission where the contribution of allophycocyanin at 660 nm is seen to be somewhat higher. The core in the mutant phycobilisomes contains only two terminal acceptor bilins, those on the two L_{CM}^{99} polypeptides, whereas the wild-type core contains four (two α^{APB} bilins and two L_{CM}^{99} bilins). The increase in 660 nm emission may be simply a consequence of the additional transfer steps between bilins on allophycocyanin subunits required for the excitation energy from any of the allophycocyanin subunits in the mutant core to reach the remaining two terminal acceptor bilins. Since the energy loss due to allophycocyanin fluorescence in the wild-type phycobilisomes is 1–2% (see Table II), the observed increase in such fluorescence in the mutant phycobilisomes represents a very small additional energy loss. The fluorescence increase represents roughly a doubling of the allophycocyanin emission, which would be consistent with the loss of half of the four approximately equivalent terminal acceptors. This interpretation is consistent with the near-identity of fluorescence decay kinetics between *apcD*$^-$ mutant and the wild-type phycobilisomes.

The L_C^8 and α^{APB} polypeptides are highly conserved in a wide variety of cyanobacterial phycobilisomes. The mutant lacking L_C^8 is at a clear disadvantage relative to the wild-type, as evidenced by the slower growth rate and decreased phycobilisome stability. This does not appear to be the case for the mutant lacking α^{APB}. The inescapable conclusion is that the conditions under which the function of α^{APB} is important have yet to be defined.

Acknowledgements

The authors would like to thank Veronica Stirewalt for assistance with the cloning and characterization of

the *apcABC* and *apcD* loci of *Synechococcus* sp. PCC 7002, and Sigurd Wilbanks for performing the amino-terminal sequence analyses. This work was supported by the Director, Office of Energy Research, Office of Basic Energy Sciences, Biological Energy Research Division, of the U.S. Department of Energy under Contract No. DE-AC03-76SF00098 (P.M. and K.S.), USPHS grant GM-31625 (D.A.B.), and NSF grants DMB-8518066 and DMB-8816727 (A.N.G.).

References

1 Glazer, A.N. (1984) Biochim. Biophys. Acta 768, 29–51.
2 Gantt, E. (1980) Int. Rev. Cytol. 66, 45–80.
3 Glazer, A.N. (1985) Annu. Rev. Biophys. Biophys. Chem. 14, 47–77.
4 Glazer, A.N., Lundell, D.J., Yamanaka, G. and Williams, R.C. (1983) Annu. Microbiol. Inst. Pasteur, 134B, 159–180.
5 Lundell, D.J. and Glazer, A.N. (1983) J. Biol. Chem. 258, 894–901.
6 Lundell, D.J. and Glazer, A.N. (1983) J. Biol. Chem. 258, 902–908.
7 Lundell, D.J. and Glazer, A.N. (1983) J. Biol. Chem. 258, 8708–8713.
8 Anderson, L.K. and Eiserling, F.A. (1986) J. Mol. Biol. 191, 441–451.
9 Gingrich, J.C., Blaha, L.K. and Glazer, A.N. (1982) J. Cell Biol. 92, 261–268.
10 Gingrich, J.C., Lundell, D.J. and Glazer, A.N. (1983) J. Cell. Biochem. 22, 1–14.
11 Bryant, D.A. (1988) In Light Energy Transduction in Photosynthesis: Higher Plant and Bacterial Models (Stevens, S.E., Jr. and Bryant, D.A., eds.), pp. 62–90, The American Society of Plant Physiologists, Rockville, MD.
12 Stevens, S.E., Jr. and Porter, R.D. (1980) Proc. Natl. Acad. Sci. USA 77, 6052–6056.
13 Stevens, S.E., Jr., Patterson, C.O.P. and Myers, J. (1973) J. Phycol. 9, 427–430.
14 De Lorimier, R., Bryant, D.A., Porter, R.D., Liu, W.-Y., Jay, E. and Stevens, S.E. Jr. (1984) Proc. Natl. Acad. Sci. USA 81, 7946–7950.
15 Sullivan, M.A., Yasbin, R.E. and Young, F.E. (1984) Gene 29, 21–26.
16 Vieira, J. and Messing, J. (1982) Gene 19, 259–268.
17 Hanahan, D. and Meselson, M. (1983) Methods Enzymol. 100, 333–342.
18 Bryant, D.A. and Tandeau de Marsac, N. (1988) Methods Enzymol. 167, 755–765.
19 Maniatis, T., Fritsch, E.F. and Sambrook, J. (1982) Molecular Cloning: A Laboratory Manual, Cold Springs Harbor Laboratory Publications, Cold Springs Harbor, New York.
20 Feinberg, A.P. and Vogelstein, B. (1983) Anal. Biochem. 132, 6–13.
21 Berger, S.L. and Kimmel, A.R. (1987) Methods Enzymol. 152, 813 pp.
22 Ausubel, F.M., Brent, R., Kingston, R.E., Moore, D.D., Seidman, J.G., Smith and Struhl, K. (1987) Current Protocols in Molecular Biology, Greene Publishing Associates, John Wiley & Sons, New York.
23 Bryant, D.A., De Lorimier, R., Lambert, D.H., Dubbs, J.M., Stirewalt, V.L., Stevens, S.E. Jr., Porter, R.D., Tam, J. and Jay, E. (1985) Proc. Natl. Acad. Sci. USA 82, 3242–3246.
24 Yamanaka, G., Glazer, A.N. and Williams, R.C. (1978) J. Biol. Chem. 253, 8303–8310.
25 Laemmli, U.K. (1970) Nature (Lond.) 227, 680–685.
26 O'Farrell, P.H. (1975) J. Biol. Chem. 250, 4007–4021.
27 Matsudaira, P. (1987) J. Biol. Chem. 262, 10035–10038.
28 Glazer, A.N., Fang, S. and Brown, D.M. (1973) J. Biol. Chem. 248, 5679–5685.
29 Hewick, R.M., Hunkapillar, M.H., Hood, L.E. and Dreyer, W.J. (1981) J. Biol. Chem. 256, 7990–7997.
30 Bryant, D.A., De Lorimier, R., Guglielmi, G., Stirewalt, V., Cantrell, A. and Stevens, S.E., Jr. (1987) In Progress in Photosynthesis Research (Biggins, J., ed.), Vol. IV, pp. 749–755, Martinus Nijhoff, Dordrecht, The Netherlands.
31 Maxson, P. (1988) Ph.D. Thesis, University of California, Berkeley. Lawrence Berkeley Laboratory Report LBL-26163.
32 Yamanaka, G., Lundell, D.J. and Glazer, A.N. (1982) J. Biol. Chem. 257, 4077–4086.
33 Lundell, D.J. and Glazer, A.N. (1981) J. Biol. Chem. 256, 12600–12606.
34 Glazer, A.N. and Bryant, D.A. (1975) Arch. Microbiol. 104, 15–22.
35 Redlinger, T. and Gantt, E. (1981) Plant Physiol. 68, 1375–1379.
36 Lundell, D.J., Yamanaka, G. and Glazer, A.N. (1981) J. Cell Biol. 91, 315–319.
37 Glazer, A.N., Chan, C., Williams, R.C., Yeh, S.W. and Clark, J.H. (1985) Science 230, 1051–1053.
38 Füglistaller, P., Mimuro, M., Suter, F. and Zuber, H. (1987) Hoppe Seyler's Biol. Chem., 368, 353–367.
39 Maxson, P., Sauer, K. and Glazer, A.N. (1988) In Photosynthetic Light-Harvesting Systems (Scheer, H. and Schneider, S., eds.), pp. 217–232, Walter de Gruyter, Berlin.
40 Zilinskas, B.A., Greenwald, L.S., Bailey, C.L. and Kahn, P.C. (1980) Biochim. Biophys. Acta 808, 52–65.
41 Mimuro, M., Lipschultz, C. and Gantt, E. (1986) Biochim. Biophys. Acta 852, 126–132.
42 Gillbro, R., Sandström, Å., Wendler, J. and Holzwarth, A.R. (1985) Biochim. Biophys. Acta 808, 52–65.
43 Suter, F., Füglistaller, P., Lundell, D.J., Glazer, A.N. and Zuber, H. (1987) FEBS Lett. 217, 279–282.
44 Houmard, J., Capuano, V., Coursin, T. and Tandeau de Marsac, N. (1988) Mol. Microbiol. 2, 101–107.